



# Tracing natural organic matter at the scale of drainage basins

Pépin-Donat B. <sup>a</sup>, Poulencard J. <sup>e</sup>, Blondel T. <sup>c</sup>, Lombard C. <sup>a</sup>, Protière M. <sup>a</sup>, Dudal Y. <sup>d</sup>, Perrette Y. <sup>e</sup>, Fanget B. <sup>e</sup>, Miège C. <sup>f</sup>, Delannoy J.-J. <sup>e</sup>, Dorioz J.-M. <sup>b</sup>, Emblanch C. <sup>c</sup>, Arnaud F. <sup>e</sup>, Giguët-Covex C. <sup>e</sup>

<sup>a</sup> *UMR SPrAM (CEA-CNRS-UJF), INAC, CEA-Grenoble, Grenoble.*

<sup>b</sup> *UMR CARRTEL, (University of Savoie-INRA), Le Bourget-du-Lac.*

<sup>c</sup> *UMR EMMAH, Laboratory of Hydrogeology of Avignon (INRA-University of Avignon), Avignon.*

<sup>d</sup> *UMR BSR (INRA-SupAgro), Montpellier.*

<sup>e</sup> *UMR EDYTEM (CNRS-University of Savoie), Le Bourget-du-Lac.*

<sup>f</sup> *UR QELY (IRSTEA), Cemagref, Lyon.*

## 2.1 - Introduction

Organic matter from plants and animals is transformed over time by two types of reaction: mineralisation and humification. These processes produce antagonistic effects: production of greenhouse gases for the first [Lugo and Brown, 1993; Raich and Potter, 1995], and synthesis of complex organic systems [Kelleher and Simpson, 2006] allowing carbon storage on Earth for the second [Lal and Bruce, 1999]. Complex organic systems resulting from humification make up what is commonly known as soil Natural Organic Matter (NOM) which is the *source* of terrestrial NOM. NOM has an extremely complex structure, it is made up of a wide variety of more or less aromatic molecules and macromolecules assembled in supramolecular architectures. To further add to the complexity, the structural properties of NOM depend on numerous parameters including,

among others, the nature of the waste from which it is produced, the mineral compounds making up the rock on which it undergoes decomposition (lithological factors), the climatic conditions, the pH conditions of the medium in which it is found, conditions linked to human activity, its depth of burial. In other words, not only is the structure of NOM extremely complex, in addition it depends on the location of its sampling site, on the surface or at a depth. In practice, we can consider that there are as many structures of organic matter as there are samples collected!

It is nevertheless crucial to characterise the flow and reactivity of natural organic matter. Indeed, NOM is the largest carbon reservoir on Earth, with a mass estimated at  $1500 \times 10^9$  tons [Batjes, 1996]. It plays a major role in the nutrient cycle within terrestrial ecosystems and between terrestrial and aquatic ecosystems due to its partial solubility. It can interact with numerous toxic organic and mineral substances [Jerzykiewicz, 2004]. Its supramolecular structure, linked to its amphiphilic nature, could explain some critical soil degradation [Poulenard *et al.*, 2004; Szajdak *et al.*, 2003]. To manage ecosystems, it is therefore necessary to better understand the dynamics and reactivity of NOM and how they depend on climate, plant coverage, hydrodynamic regimes, lithology and human activity. To be complete, NOM should be studied at various scales, from the molecular to the scale of the Earth as a whole. However, as drainage basins represent a scale covering both terrestrial life and human management, we chose to work at this intermediate scale.

As the structure of NOM is highly complex and variable it is absolutely impossible to determine it, and because of this, reactive properties and flow must be studied without reference to its structure. This type of study would be impossible with classical methods. However, NOM can be studied using “tracing” methods. These methods do not attempt to precisely determine the structures of the organic systems studied but use a fingerprint linked to a tracer to identify major sub-structural types present in the overall system. The tracers exploited must be ubiquitous, stable over time and space, capable of distinguishing between relatively similar sub-structures (i.e., be discriminative), and easy to detect. The markers currently used do not combine all these characteristics. They can be classified in two major categories: “analytical” markers (atoms or molecules), these are very discriminative but impossible to monitor over large space and time scales [Peters, 1993; Simoneit, 2002; Jacob *et al.*, 2008; Blyth *et al.*, 2008] and

spectroscopic markers (IR, UV-Vis., 3D fluorescence), which are easy to track over large spatial scales but are not very discriminative [Stedmon *et al.*, 2003; Sierra *et al.*, 2005]. Existing tracing methods therefore cannot be used to study the structure, reactivity and dynamics of NOM over extended spatial and time scales.

EPR tracing involves the use of new tracers: semiquinone-type free radicals. These radicals are generated and trapped within aromatic structures in NOM during the humification process. This process mainly consists in oxidation of lignin followed by a loss of aliphatic and carboxylic groups to produce polyphenol units. These units are subsequently oxidised to produce quinone units, passing through semiquinone intermediates. Semiquinone free radicals are ubiquitous, stable and readily detectable by EPR. They have been extensively used since the 1960s to characterise the degree of humification of NOM [Steelink and Tollin, 1967; Senesi, 1990; Nickel-Pépin-Donat *et al.*, 1990; Yabuta *et al.*, 2005; Saab and Martin-Neto, 2008]. Schnitzer suggested that they could be used as tracers as early as 1972 [Schnitzer and Khan, 1972], but the idea was never followed through or implemented.

In this chapter, we first show that the EPR spectrum of semiquinone radicals differentiate between NOM from neighbouring soils and even from different levels within the same soil. We then show that tracing of these radicals by EPR can be used to monitor the transfer of NOM from soils in a drainage basin to its hydrological system, from this system to its spillway, and even down to their natural recorders such as sediments and speleothems (stalagmites). We tested the efficacy of this method on three clearly differentiated drainage basins and compared the results to those given by independent studies applying other techniques. The results show that this tracing method has great potential as a tool to help with management of drainage basins. Numerous applications can now be imagined, and as an example we show how it can help to determine the catchment area and the residence time for drinking water in karst formations.

## **2.2 - Transformation and transfer of natural organic matter**

On Earth, the different forms of natural organic matter can be classified as a function of their ages:

- ▷ recent NOM, present in soils and spring waters. Their age varies between 1 year and a few thousand years,

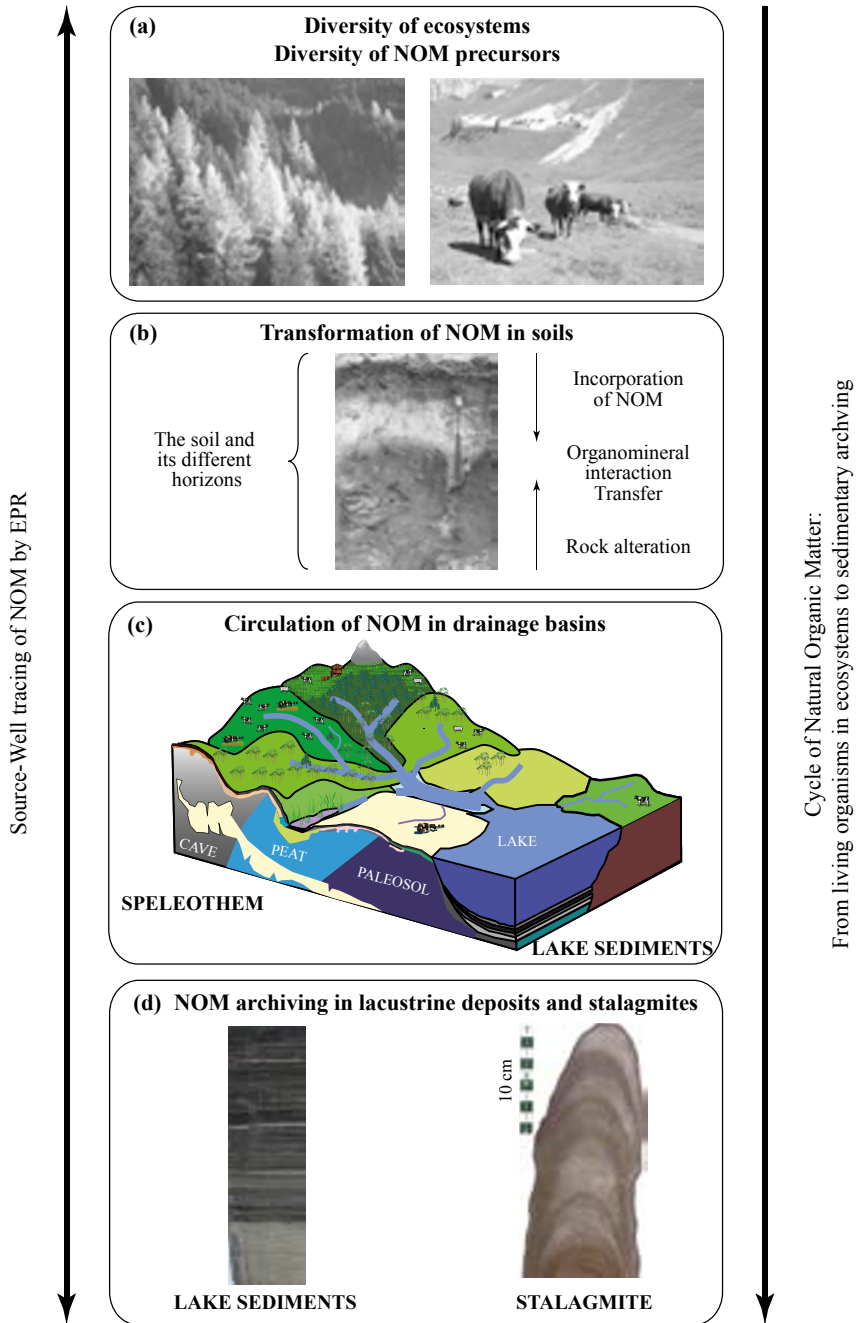
- ▷ NOM from natural recorders such as sediments, peat, stalagmites, ice. Their age ranges from several hundred years to several hundred thousand years,
- ▷ fossil NOM in coal and petrol, which is between a few hundred thousand and several billion years old,
- ▷ extraterrestrial NOM that is found in meteorites.

In this chapter we are interested in the first two categories. EPR also provides information on the structural and reactive properties of fossil NOM [Nickel-Pépin-Donat *et al.*, 1990; Pépin-Donat and Brunel, 1994] and on extraterrestrial organic matter. Chapter 7 in this volume describes how EPR contributes to the study of primitive, terrestrial and extraterrestrial, carbonaceous matter in the context of the search for the origins of life.

The variety of NOM precursors, which depends on the type of vegetation and the presence of agricultural or pastureland activities, results in diverse ecosystems (figure 2.1a). The progressive incorporation of these precursors into soils and their interaction with the products of the alteration of rocks lead to the formation of layers of NOM which are more or less parallel to the surface, known as *soil horizons*. Each horizon can be considered to present a certain homogeneity in terms of chemical and physical properties (density, pH, ionic conduction, colour, etc.) and the state of transformation of the NOM (figure 2.1b). NOM can be mobilised by the water circulating in drainage basins, in particulate form (alone or in organo-metallic complexes), in colloidal form, or as solutes. NOM from different sources (various precursors, different horizons) circulate in drainage basins where they are mixed together (figure 2.1c). In some conditions, NOM can accumulate in datable “sedimentary archives” (lake sediments, stalagmites) (figure 2.1d).

Given the complexity of the structures and reactivity of NOM, it initially appears extremely difficult to reconstitute their transfer. However, we will see that EPR tracing efficiently contributes to overcoming this hurdle and provides information on a certain number of basic processes:

- ▷ the dynamics of NOM transformation in soils, which has significant consequences on the mechanisms through which organic carbon is stored,
- ▷ the dynamics of transfer into water. This would make it possible, for example, to determine the origin of NOM which can alter the water’s quality,
- ▷ the formation of paleo-environments and paleo-ecosystems, by revealing the origin of NOM archived in sediments and/or stalagmites.



**Figure 2.1** - (a) diversity of NOM precursors, (b) incorporation and transformation of NOM precursors in soil horizons, (c) circulation of NOM from soils to water, (d) archiving NOM in natural recorders, sediments, peat, ice, stalagmite (represented here).

### 2.3 - EPR signature of natural organic matter

The EPR spectrum recorded at room temperature for a sample of NOM results from the superposition of the signals produced by its semiquinone radicals. It depends on the nature, organisation and dynamics of the aromatic entities present in complex organic structures. When the sample contains only one type of these structures, its spectrum contains a single line which can be characterised by four parameters: its position, defined by the  $g$  factor; its shape, defined by the Lorentzian percentage ( $\%L$ ) of a linear combination of Lorentzian and Gaussian; its peak-to-peak width  $\Delta B_{pp}$  expressed in mT; and its concentration  $[I]$  in number of spins per unit of organic carbon mass. The  $g_{iso}$  factor for semiquinone radicals is between 2.0028 and 2.0055 [Riffaldi and Schnitzer, 1972; Barančíková *et al.*, 1997; Yabuta *et al.*, 2005] and its value is sensitive to the chemical structure into which the electron is delocalised. For example, the  $g_{iso}$  factors for the radicals which have notable spin density on oxygen, nitrogen or sulfur atoms are higher than those of radicals where the spin density is mainly delocalised on carbon atoms [Volume 1, section 4.2.2]. The shape of the line, its width and the spin concentration are also sensitive to the environment of the unpaired electron, but not in a simple manner. Additional experiments, such as those described in chapter 7 for the investigation of primitive carbonaceous matter, would be necessary to obtain detailed information on the structure and dynamics of these organic structures. But, for the needs of the application described in this chapter, we can consider that the set of parameters ( $g$ ,  $\%L$ ,  $\Delta B_{pp}$ ,  $[I]$ ) constitutes a characteristic *signature* of the nature and dynamics of the complex organic matter in which the electrons are trapped. As the EPR lines of all the samples of NOM sampled in this study have a *Lorentzian* shape, the ( $\%L$ ) parameter will not be used here.

When the sample contains several types of complex organic matter, the spectrum is a superposition of the components corresponding to the different types. The characteristic parameters can be readily determined by simulating the experimental spectrum using a sum of “pure” components. It is possible to determine the absolute number of spins  $[I_i]$  corresponding to each component, but this calculation is only justified when it is useful to quantify the masses of the different types of NOM. This is not the case in the methodological study presented here, and we will therefore neglect this parameter. In contrast, the *relative intensities* of the different components of the spectrum, which are very easy to determine, are very important in the context of this study aiming to simply visualise *variations*

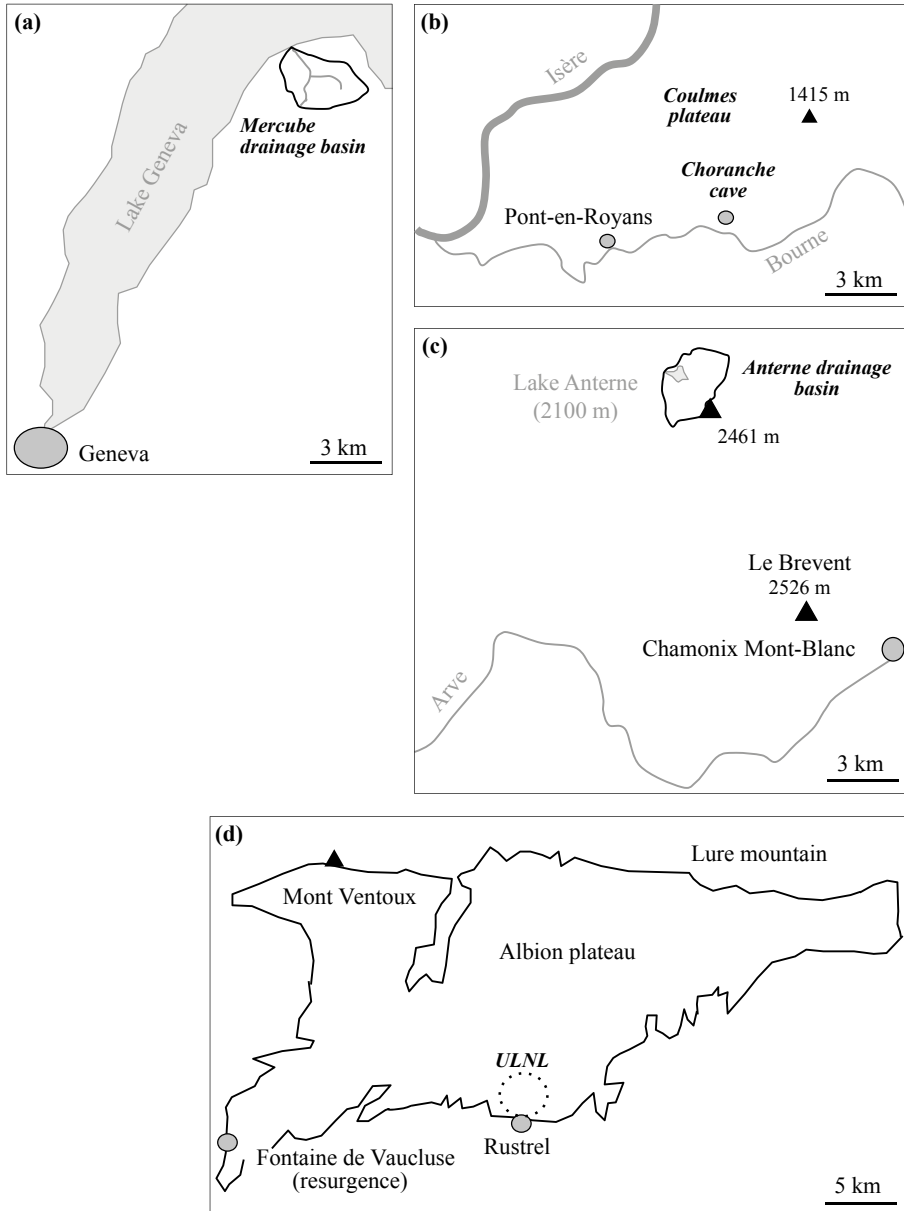
in composition of the NOM during its transformation and transfer. We will see that it is convenient to use a “barcode” in which each component is represented by a coloured bar, the height of which is proportional to its relative intensity.

## 2.4 - Study areas and protocol applied

### 2.4.1 - Description of the drainage basins studied

In figure 2.2 we have indicated the sites of the three drainage basins which we used to test the EPR tracing method, as well as the Fontaine de Vaucluse basin which was the object of a specific application of this method.

- ▷ The study of the Mercube river drainage basin **(a)** was used to test tracing of NOM from soils (sources of NOM) down to superficial waters, within the water network and finally to the basin’s spillway. This small river drains a 302-ha basin and flows into lake Geneva close to Yvoire in Haute-Savoie. The basin has gentle slopes. Part of the basin is characterised by the presence of clay-rich soils and a high-altitude layer where the water stagnates at the surface during the winter. This zone, which is difficult to exploit agriculturally is occupied by a forest (123 ha). The remainder of the basin is composed of a one-metre deep, well drained silt-rich soil. These soils are used to produce wheat and corn (120 ha) or as grassland (50 ha).
- ▷ The **(b)** Coulmes/Choranche (Isère) and **(c)** Anterne (Haute-Savoie) sites were studied to test the persistence of EPR signatures and their relevance for NOM tracing from soils to waters, and from waters to natural recorders (speleothems and lake sediments) (figures 2.1c and 2.1d). The site of Coulmes/Choranche corresponds to a karst system in the Vercors mountain range. The Coulmes plateau, at an altitude of between 800 and 1 400 m, is covered with a gradient of vegetation from a lower-altitude forest of oaks and box trees to a mountain forest of spruce and fir. This environment has developed on hard limestone rocks. The dominant soils are characterised by the organic matter accumulated on the exposed hard limestone. Brown forest soils develop in dolines where clay has accumulated. The underground karst rivers fed by this plateau flow into the Choranche caves. The site of Anterne, in Sixt Nature Reserve (Haute-Savoie), corresponds to a small subalpine drainage basin (2.5 km<sup>2</sup>) which feeds into a lake located at an altitude of 2 063 m. This drainage basin is currently covered by alpine grasslands of graminæa which is mainly developed on brown soils. However, on very steep slopes, little-evolved soils are found on schist and dark earth. A few peaty zones are present around the lake.



**Figure 2.2** - Localisation of the different basins and sites studied: (a) “Mercube” basin, (b) Coulmes/Choranche basin, (c) Anterne basin, (d) Fontaine de Vaucluse basin. The localisation of the Underground Low-noise laboratory (ULNL) where sampling was performed for this basin is shown.



- ▷ Fontaine de Vaucluse is one of the most extensive European karstic sources, with a mean flow-rate of  $23 \text{ m}^3 \text{ s}^{-1}$ . It is the main egress for a 1500 m thick limestone formation which extends over 1115 km<sup>2</sup>. We studied the Rustrel site (**d**) which is part of its catchment area. It is located in a Mediterranean karstic environment. This study aimed to test EPR tracing of NOM from soils to subterranean water and to demonstrate its application to determine the catchment area and the residence time for drinking water in karst formations. The sampling site is shown in figure 2.6. The Rustrel-Apt area underground low-noise laboratory (ULNL) provides privileged access to several permanent flows from the “unsaturated zone” (where not all the empty spaces in the karst are filled with water) for the Fontaine de Vaucluse hydrosystem. The ULNL is composed of subterranean galleries which randomly split up the karstic network. For this study, a permanent flow located at 440 m under the surface (figure 2.6a) was monitored between December 2006 and December 2007. In this area, only two types of organic matter sources are present at the surface [Emblanch *et al.*, 1998]: sloping soil covered by disperse shrub-based (S1a) and grassy (S1b) vegetation, and soil that develops on the plateau (S2), which is covered by a forest of holm oaks.

#### 2.4.2 - Sample preparation

Soil samples from all of the areas studied were sampled by a soil survey performed on the four basins. Their preparation was limited to grinding and sieving to 2 mm.

Sediments from the Anterne basin were collected using sediment traps installed in the rivers and at the bottom of the lake at 13 m depth. Sediments were also extracted from a core of lacustrine deposits. Here, we present the results for deposits sampled at a core-depth of 28–29 cm, dating from around 1950.

In the Choranche caves, the sub-current (growth later than 1950) “stalagmitic floor” was sampled in the subterranean river. This is a carbonaceous formation similar to stalagmites but which constitute a surface layer which has formed at the bottom of the cave.

Aqueous extracts from soils of the karstic Coulmes plateau were prepared in the laboratory using a soil/solution ratio of 1/10 and orbital agitation at 300 revolutions per minute for 4 hours. They were filtered at 0.2 μm.

Waters from rivers were collected in the forest and agricultural sub-basins of the Mercube drainage basin during a winter low-flow period. Samples were also collected at the level of the spillway into lake Geneva.

Monthly sampling of the subterranean flow in the ULNL gallery was performed over the 2006–2007 hydrological cycle. All samples of natural water were gently evaporated at 40 °C to produce a dry residue (around 50 L filtered at 0.45 µm).

### **2.4.3 - Recording and simulation of EPR spectra**

Solid samples (a few milligrammes) were placed in 3-mm diameter quartz tubes. Aqueous solutions were injected into 0.2-mm diameter quartz capillary tubes. EPR spectra were recorded at room temperature on an X-band EMX Bruker spectrometer, with a non-saturating power of 20 mW. The magnetic field and microwave frequency were measured independently to determine the  $g$  factor with a precision of  $\pm 0.0002$ . The number of components present in the spectrum and the parameters characterising them ( $g$ ,  $\Delta B_{pp}$ ,  $[I]$ , see section 2.3) were determined by simulating the part of the spectrum corresponding to semiquinone-type radicals thanks to a specifically-developed programme. We then determined the barcodes by attributing a height proportional to its relative intensity to each component.

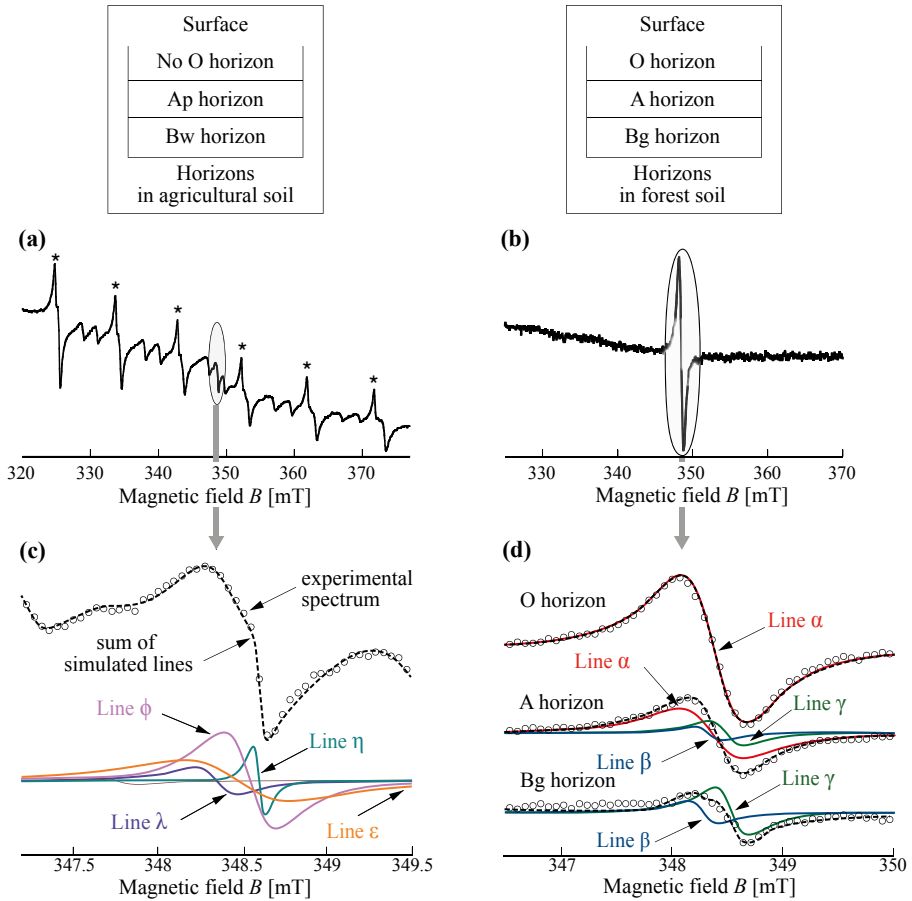
## **2.5 - Assessing the EPR tracing method**

In this section, we describe the studies which demonstrated the potential of the EPR tracing method. To better appreciate their field of application, they were performed on 3 very different drainage basins.

### **2.5.1 - EPR signatures can distinguish between different soil types and between horizons in a single soil**

The EPR spectra for soil samples collected in agricultural and forest areas of the Mercube drainage basin are represented in figure 2.3. Figures 2.3a and 2.3b, respectively, show the spectra for the Bw horizon in agricultural soil and for the O horizon in forest soil recorded over around 60 mT. Figure 2.3c zooms in on the  $g \sim 2$  region of the spectrum which corresponds to the semiquinone radicals of the Bw horizon and shows its simulation. Figure 2.3d shows how the spectrum for NOM in forest soil changes as a function of depth of sampling. The intensity of a broad line  $\alpha$  specific to the surface horizon can be observed to

decrease with depth, whereas several narrower lines  $\beta$  and  $\gamma$  appear. Similarly, for agricultural soil, the intensity of the broad line  $\epsilon$  specific for the Ap horizon (figure 2.4a) is considerably decreased in the Bw horizon, but a narrower line  $\phi$  appears (figure 2.3c).

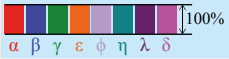
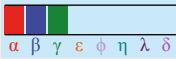
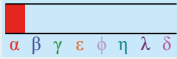
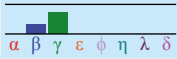
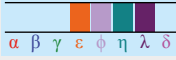

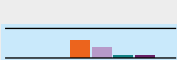
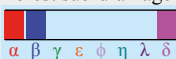







**Figure 2.3** - X-band spectra for: (a) the Bw horizon in agricultural soil (asterisks indicate lines attributed to  $\text{Mn}^{2+}$  ions), (b) the O horizon for forest soil, recorded over 60 mT, the  $g \sim 2$  region characteristic of NOM is presented in detail in (c) for the Bw horizon of agricultural soil and in (d) for the O, A and Bg horizons of forest soil. The experimental spectra (circles), their simulation (black dashes) and their various components are represented. The parameters used in the simulation and associated barcodes are indicated in table 2.1. Given the value of their  $g$  factor, some signals which appear during the simulation cannot be attributed to the NOM. They are therefore not listed.

This *narrowing* of the lines as we move away from the surface of the soil is attributed to *maturation* of the NOM [Barančíková *et al.*, 1997], in agreement

with data published on the evolution of NOM in soils [Schulten and Schnitzer, 1997; Schulten and Leinweber, 2000; Leenheer, 2007]. The parameters used to simulate the spectra and associated barcodes can be found in table 2.1.

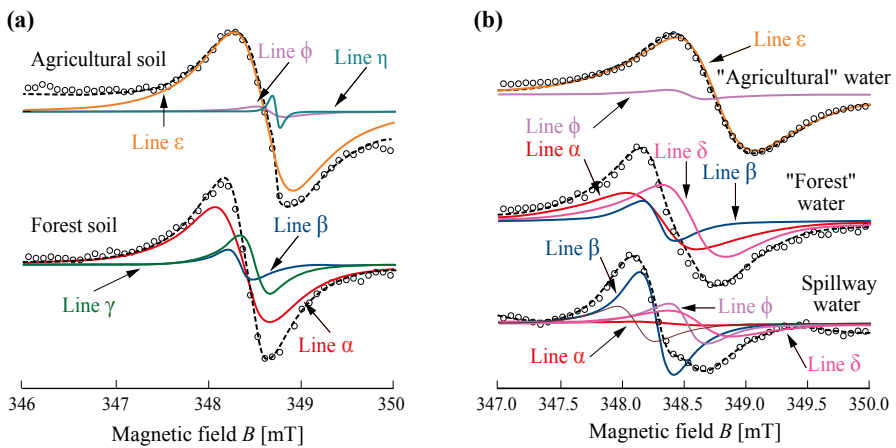
**Table 2.1** - Simulation parameters and barcodes for soils and waters for the Mercube drainage basin.

 <b>Overall signature for MERCUBE drainage basin</b>						
Soils and their EPR signature	Line	$g_{iso}$ factor	Linewidth $\Delta B_{pp}$ [mT]	Relative intensity [%]	Quantification of EPR signatures: «barcodes»	
Forest «gleyic cambisol» 	<b>O</b>	$\alpha$	2.0048	0.59	100	
		<b>A</b>	$\alpha$	2.0048	0.59	82
	$\beta$		2.0053	0.28	5	
	$\gamma$		2.0042	0.31	13	
	<b>Bg</b>	$\beta$	2.0053	0.28	27	
$\gamma$		2.0042	0.31	73		
Agricultural «cambisol» 	<b>Ap</b>	$\epsilon$	2.0036	0.64	98	
		$\phi$	2.0032	0.31	1.7	
		$\eta$	2.0029	0.08	0.3	
	<b>Bw</b>	$\epsilon$	2.0036	0.64	57.9	
		$\phi$	2.0032	0.31	34.5	
		$\eta$	2.0029	0.08	1.5	
$\lambda$	2.0043	0.25	6.1			
<b>Waters and their EPR signature</b>						
Forest sub-drainage basin 	$\alpha$	2.0048	0.59	48		
	$\beta$	2.0053	0.28	7.5		
	$\delta$	2.0036	0.51	44.5		
Agricultural sub-drainage basin 	$\epsilon$	2.0036	0.64	98		
	$\phi$	2.0032	0.31	2		
Spillway for the entire drainage basin 	$\alpha$	2.0048	0.59	7.1		
	$\beta$	2.0053	0.28	44.1		
	$\phi$	2.0032	0.31	19		
	$\delta$	2.0036	0.51	29.8		

The capacity of the EPR signatures to distinguish between different soil types and the horizons in a single soil will be confirmed by studies performed on the three other sites. EPR can thus be used for a detailed study of NOM transfers within drainage basins.

### 2.5.2 - EPR signatures can be used to monitor the transfer of NOM of various origins to hydrographic networks

Analysis of the spectra in figure 2.4 demonstrates the capacity of EPR tracing to monitor the transfer of NOM from soils to the hydrographic network down to the spillway for the Mercube drainage basin. Figure 2.4a shows spectra for type A horizons for the soils from agricultural and forest sub-basins, and figure 2.4b shows those for the dry residues from water collected in these two sub-basins and at the level of the spillway into lake Geneva.



**Figure 2.4** - EPR spectra recorded in the  $g \sim 2$  region characteristic of NOM.

(a) Ap horizon for agricultural soil and A horizon for forest soil, (b) dry residue from water sampled in the agricultural and forest sub-basins and at the level of the spillway into lake Geneva. The experimental spectra (circles), their simulation (black dashes) and their various components are represented. The parameters used in the simulation and associated barcodes are indicated in table 2.1. Given the value of their  $g$  factor, some signals which appear during the simulation cannot be attributed to NOM. They are therefore not listed.

Comparison of these spectra leads to the following conclusions:

- ▷ Spectra for water samples collected in the forest and agricultural sub-basins include some of the lines detected in the corresponding soils: lines  $\epsilon$  and  $\phi$  characteristic of the agricultural soil are found in “agricultural” waters and lines  $\alpha$  and  $\beta$  characteristic of the forest soil are detected in that for “forest” waters. All four lines are also found in water from the spillway into lake Geneva.
- ▷ Line  $\gamma$  characteristic of the forest soil is absent from “forest” water: it is said not to be *water available*.

- ▷ Conversely, on the spectrum for the water from the forest sub-basin and the spillway a line  $\delta$  is observed which is not detected in any of the soils sampled. This may be a result of non-exhaustive sampling of the soils, the presence of a native source of NOM in the waters, or transformation of a type of NOM in the soil during its transfer.

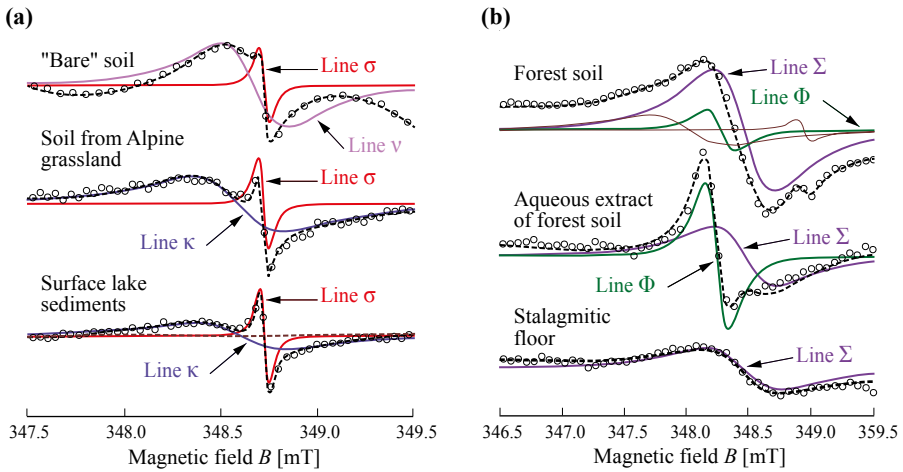
The presence of characteristic lines specific to the forest and agricultural sub-basins in the spectrum of the waters collected from the spillway is coherent with the results of independent studies [Jordan-Meille *et al.*, 1998; Jordan-Meille and Dorioz, 2004]. It reveals the power of the EPR tracing method to simply and effectively study the transfer of the major types of NOM present in a drainage basin.

### ***2.5.3 - EPR signatures can be used to trace transfer of NOM from soils to natural recorders***

The studies carried out on the sites of lake Anterne and Coulmes/Choranche confirmed that EPR signatures can distinguish between different types of soil; it is thus possible to determine the origin of the NOM present in natural recorders: sediments and speleothems.

**Anterne basin.** We traced the NOM from the soils to the river and lake sediments. Figure 2.5a shows examples of spectra and their simulations, and all the results are presented in table 2.2. The main conclusions are as follows:

- ▷ A very narrow line  $\sigma$  is detected in all samples, whether soils or river or lake sediments. This line reveals the presence of an extensively matured NOM [Senesi and Steelink, 1989], probably derived from the mature organic matter trapped in sedimentary rocks.
- ▷ In the case of river deposits, in addition to line  $\sigma$ , a broader line,  $\nu$ , is observed. This line is only found in the spectrum of little-evolved soils (lithosols), bare soil or under sparse vegetation, which are easily eroded. The presence of NOM from these soils in river sediments is therefore not unexpected.
- ▷ In the case of samples collected in sediment-traps placed at the bottom of the lake or in cores of lacustrine deposits, line  $\nu$  is replaced by another line,  $\kappa$ . This line is detected in the spectrum for hydromorphic brown soils, which are water-logged for part of the year and are abundant on riverbanks. Riverbank sapping phenomena and regressive erosion of these formations are effectively observed in the basin.




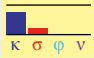







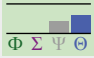



**Figure 2.5** - Experimental spectra (circles), simulations (black dashes) and different components for **(a)** Anterne basin: bare soil, brown soils of Alpine grassland and surface sediments from lake Anterne, **(b)** brown forest soil from the Coulmes plateau, its aqueous extract, stalagmitic floor from Choranche cave. The simulation parameters and associated barcodes are indicated in table 2.2.

EPR tracing therefore reveals that the NOM for river and lake sediments are derived from different soils: bare and little-evolved soils for river sediments, more evolved soils from the banks of waterways for lake sediments. Sediments from bare soils do not appear to accumulate in deltas, which explains why they contribute little to the sediments in the centre of the lake. This result is in agreement with the conclusion of a recent geochemical study (mineral and organic) comparing current soils to lake sediments from the holocene period (last 12,000 years) [Giguet-Covex *et al.*, 2011].

**Choranche karst basin.** The spectrum produced by the sample collected in the stalagmitic floor in the Choranche caves consists of a single line  $\Sigma$  (figure 2.5b). The same signature is found in the spectrum produced by forest soils from the Coulmes plateau which covers these caves, as well as that of the aqueous extract prepared in the laboratory. However, this line is completely absent from the spectrum produced by organic soils developed on limestone and their aqueous extracts. These results indicate that the main source of NOM in the stalagmitic floor is brown soil. Without anticipating the significance of these results for our understanding of how drainage basins function, a study of which will be published later, we can already observe that EPR can be used to monitor NOM from soils to sediments and from soils to speleothems, through water-based

transfer. This conclusion shows the potential of EPR tracing to monitor NOM in paleo-environments.

**Table 2.2** - Simulation parameters and barcodes for waters and sediments from the Anterne and Choranche drainage basins.

 <b>Overall signature for main types of NOM detected at ANTERNE</b>					
Soils and their EPR signatures	Line	$g_{iso}$ factor	Linewidth $\Delta B_{pp}$ [mT]	Relative intensity [%]	Quantification of EPR signatures: «barcode»
«Alpine grassland sol» : Gleyic cambisol	$\kappa$	2.0034	0.47	81	
	$\sigma$	2.0029	0.05	19	
«Peat sol» : Histosol	$\phi$	2.0041	0.58	99.8	
	$\sigma$	2.0029	0.05	0.2	
«Bare sol» : Regosol	$\nu$	2.0032	0.35	94	
	$\sigma$	2.0029	0.05	6	
<b>Sediments and their EPR signatures</b>					
Core sediments	$\kappa$	2.0034	0.47	96	
	$\sigma$	2.0029	0.05	4	
Sediments trapped in the lake	$\kappa$	2.0034	0.47	96	
	$\sigma$	2.0029	0.05	4	
Sediments trapped in the flow	$\nu$	2.0032	0.35	90	
	$\sigma$	2.0029	0.05	10	
 <b>Overall signature for main types of NOM detected at CHORANCHE</b>					
Soils and their EPR signatures	Line	$g_{iso}$ factor	Linewidth $\Delta B_{pp}$ [mT]	Relative intensity [%]	Quantification of EPR signatures: «barcode»
«Grassland cambisol»	$\Psi$	2.0030	0.45	93	
	$\Theta$	2.0049	0.29	7	
Water extracted from the «grassland cambisol»	$\Psi$	2.0030	0.45	39	
	$\Theta$	2.0049	0.29	61	
«Forest cambisol»	$\Phi$	2.0048	0.18	7	
	$\Sigma$	2.0033	0.5	93	
Water extracted from the «forest cambisol»	$\Phi$	2.0048	0.18	25	
	$\Sigma$	2.0033	0.5	75	
Stalagmitic floor	$\Sigma$	2.0033	0.5	100	

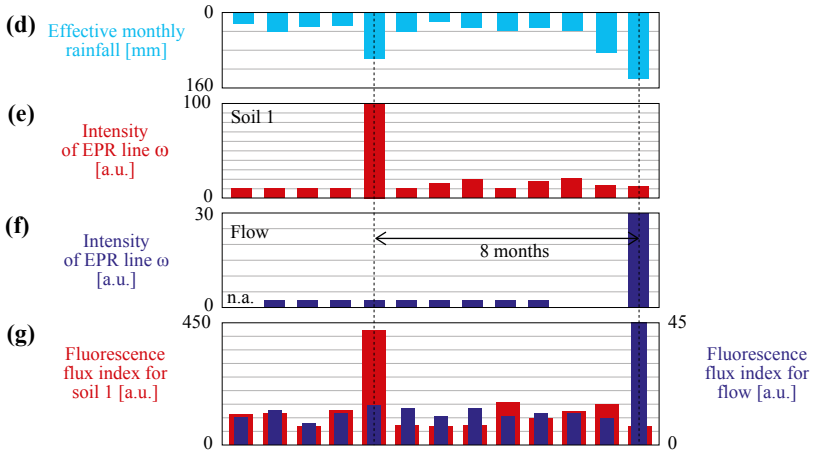
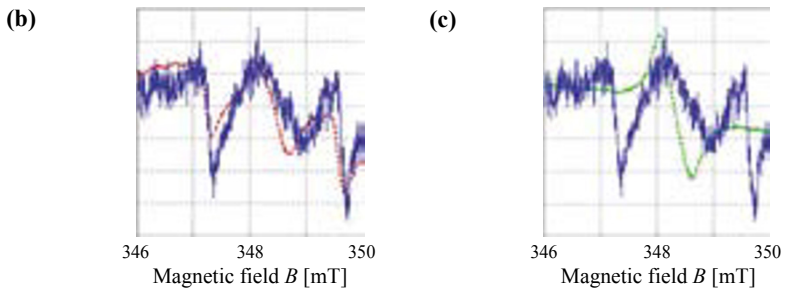
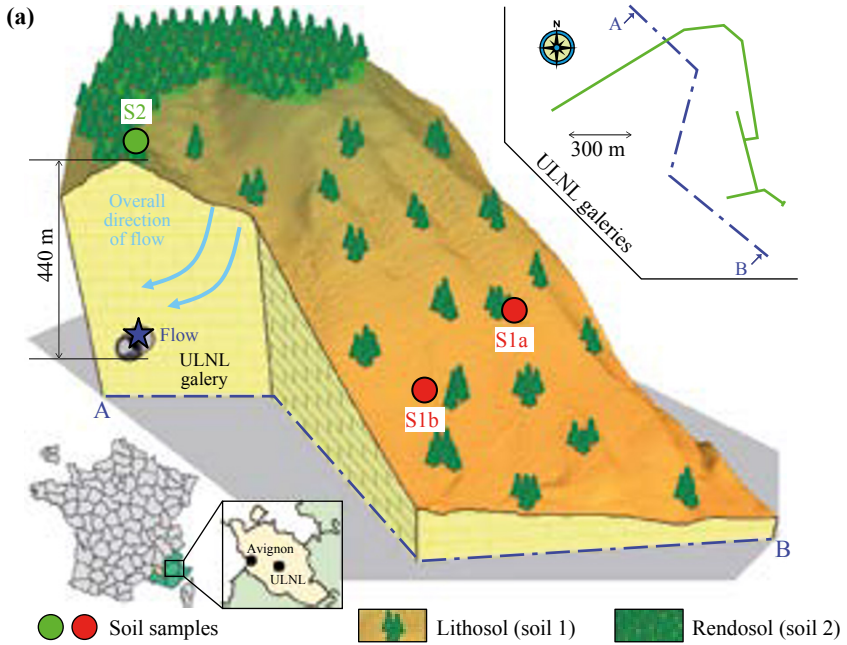


## 2.6 - Example of application of EPR tracing: identification of the inflow basin and the residence time for water in a karst formation

The aim of this study was to use EPR tracing to determine the inflow zone and the residence time for drinking water from the karstic site of Fontaine de Vacluse, and to compare the results to those given by other methods which are much more difficult to implement.

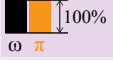


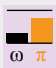

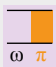
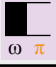
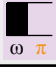
As indicated in section 2.4.1, between December 2006 and December 2007 we collected two types of soil samples, S1 and S2, which exist on this site, and water which flows at 440 m underground in the ULNL laboratory. The EPR spectrum produced by a sample of water was compared to that obtained for soils S1 and S2 in figures 2.6b and 2.6c. The simulation parameters and associated barcodes are indicated in table 2.3. Analysis of all these results leads to the following conclusions:

- ▷ The EPR spectrum for water is very similar to that for soil S1 (the spectra for soils S1a and S1b are identical) and very different from that of soil S2. More precisely, the simulation shows that the spectrum for water only has a single line  $\omega$  due to NOM; the spectrum for S1 includes the line  $\omega$  and another line  $\pi$ , whereas the spectrum for S2 contains only line  $\pi$ . We can deduce that lithosol 1 belongs to the catchment basin for the flow studied. This result is entirely coherent with the external structure of the network of faults (figure 2.6a).
- ▷ Absence of the line  $\pi$  from the water spectrum shows that it is due to a type of NOM which has a very low potential for transfer to water. This low transferability may reflect low solubility, or strong adsorption or biodegradation.
- ▷ During 2007, the intensity of the line  $\omega$  in the spectrum for soil S1 passes through a very marked maximum in the month of April (figure 2.6e). This peak of NOM is due to the heavy precipitation which occurred during that particular month (figure 2.6d), but it was only observed in the flow of subterranean water when significant infiltration occurred in December 2007, i.e., *8 months later* (figure 2.6f). This result allows us to propose a transit time for water within this karstic system of around eight months, which is in perfect agreement with the results of a fluorescence study shown in figure 2.6g [Blondel *et al.*, 2010]. It should be noted that the hypothesis of *instantaneous infiltration* of meteoritic waters towards the outlet in December 2007 is not compatible with the presence of magnesium at relatively high concentrations ( $4.14 \text{ mg L}^{-1}$ ) and very low concentrations of total organic carbon ( $0.8 \text{ mg L}^{-1}$ ) in samples collected at this time [Batiot *et al.*, 2003].



**Figure 2.6** - (a) Localisation of the ULNL laboratory and its network of faults, (b) comparison of EPR spectra for water flow (continuous line) and S1 soil (dashed line), (c) comparison with spectra for S2 soil (dashed line). The following figures show the monthly variations for different parameters between December 2006 and December 2007, (d) rainfall, (e) intensity of line  $\omega$  for soil S1, (f) intensity of line  $\omega$  for water, (g) fluorescence index for soil S1 (red) and outflow of water (purple). Simulation parameters and associated barcodes can be found in table 2.3. [From Blondel *et al.*, 2010]

**Table 2.3** - Simulation parameters and barcodes for Fontaine de Vaucluse soils and waters.

Overall signature for main types of NOM at FONTAINE DE VAUCLUSE					
Soils and their EPR signatures	Line	$g_{iso}$ factor	Linewidth $\Delta B_{pp}$ [mT]	Relative intensity [%]	Quantification of EPR signatures: "barcodes"
Soil 1a 	$\omega$	2.0040	0.62	39	
	$\pi$	2.0046	0.52	61	
Soil 1b 	$\omega$	2.0040	0.62	22	
	$\pi$	2.0046	0.52	78	
Soil 2 	$\pi$	2.0046	0.53	100	
Sampled water (see fig. 2.6) 	$\omega$	2.0040	0.62	100	

## 2.7 - Conclusion

In this chapter, we have described the first studies of EPR tracing of natural organic matter performed at the scale of drainage basins. The representation of the relative intensities of the different components of the spectrum by a "barcode" facilitates tracking of different types of NOM, from the soils of the drainage basins to natural recorders such as sediments and speleothems. This tracing method can be used to study the dynamics and reactivity of NOM at this scale, it can also be applied to paleo-environments. This novel method can also be used to obtain information on the impact of terrestrial organic matter on lacustrine ecosystems. For all these reasons, we consider that it provides a useful tool, well adapted to the management of drainage basins. In addition, comparison of variations in the EPR signatures due to the effect of various constraints

(chemical, UV radiation,  $\gamma$ , etc.) to those obtained by other techniques could be used to develop a *bank of EPR signatures* for NOM associated with their main structural and reactive characteristics. More sophisticated EPR studies (ENDOR, pulsed EPR) could also be used to obtain more detailed information on the structure of the radicals present in the different types of NOM, but this would detract from the simplicity and rapidity of the method which are its main advantages and which make it applicable at large scales of time and space.

## References

- BARANČIKOVÁ G., SENESI N. & BRUNETTI G. (1997) *Geoderma* **78**: 251-266.
- BATIOU C., EMBLANCH E. & BLAVOUX B. (2003) *Comptes Rendus Geoscience* **335**: 205-214.
- BATJES NH. (1996) *European Journal of Soil Science* **47**: 151-163.
- BINET L. *et al.* (2002) *Geochimica Cosmochimica Acta* **66**: 4177-4186.
- BLONDEL T. *et al.* (2010) *Isotopes in Environmental and Health Studies* **46**: 27-36.
- BLYTH A.J. *et al.* (2008) *Quaternary Science Reviews* **27**: 905-921.
- EMBLANCH C. *et al.* (1998) *Geophysical Research Letter* **25**: 1459-1462.
- GIGUET-COVEX C. *et al.* (2011) *The Holocene* **29**: 651-665.
- JACOB J. *et al.* (2008) *Journal of Archaeological Science* **35**: 814-820.
- JERZYKIEWICZ M. (2004) *Geoderma* **122**: 305-309.
- JORDAN-MEILLE L., DORIOZ J.M. & WANG D. (1998) *Agronomie* **18**: 5-26.
- JORDAN-MEILLE L. & DORIOZ J.M. (2004) *Agronomie* **24**: 237-248.
- KELLEHER B.P. & SIMPSON A.J. (2006) *Environmental Science and Technology* **40**: 4605-4611.
- LAL R. & BRUCE J.P. (1999) *Environmental Science and Policy* **2**: 177-185.
- LEENHEER J.A. (2007) *Annals of Environmental Science* **1**: 57-68.
- LUGO A.E. & BROWN S. (1993) *Plant and Soil* **149**: 27-41.
- NICKEL-PÉPIN-DONAT B., JEUNET A. & RASSAT A. (1990) "ESR study of the structure, texture and reactivity of the coals and coal macerals of the CERCHAR-GRECO minibank" in *Advanced Methodologies in Coal Characterization*, CHARCOSSET H., NICKEL-PÉPIN-DONAT B., eds, Elsevier, Amsterdam.
- PÉPIN-DONAT B. & BRUNEL L.C. (1994) *Journal de Chimie Physique* **91**: 1896.
- PETERS K.E., WALTERS C.C. & MOLDOWAN J.M. (1993) "Biomarkers and Isotopes in the Environment and Human History" in *The Biomarker Guide* Cambridge University Press.
- POULENARD J. *et al.* (2004) *European Journal of Soil Science* **55**: 487-496.
- RAICH J.W. & POTTER C.S. (1995) *Global Biogeochemical Cycles* **9**: 23-26.
- RIFFALDI R. & SCHNITZER M. (1972) *Soil Science Society of America Proceeding* **36**: 301-305.
- SCHULTEN H.-R. & SCHNITZER M. (1997) *Soil Science* **162**: 115-130.
- SAAB S.C. & MARTIN-NETO L. (2008) *Journal of the Brazilian Chemical Society* **19**: 413-417.
- SCHNITZER M. & KHAN S.U. (1972) *Humic substances in the environment*, Marcel Dekker, New York.
- SCHULTEN H.-R. & LEINWEBER P. (2000) *Biology and Fertility of Soils* **30**: 399-432.

- SENESI N. & STEELINK C. (1989) "Application of ESR spectroscopy to the study of humic substances" in *Humic Substances II: In Search of Structure* Hayes, M.H.B., MacCarthy P., Malcolm R.L., Swift R.S., eds, Wiley, New York.
- SENESI N. (1990) "Application of electron spin resonance (ESR) spectroscopy in soil chemistry" in *Advances in Soil Science*, Hayes, M.H.B., MacCarthy P., Malcolm R.L., Swift R.S., eds, Wiley, New York.
- SIERRA M.M.D. *et al.* (2005) *Chemosphere* **58**: 715-733.
- SIMONEIT B.R.T. (2002) *Applied Geochemistry* **17**: 129-162.
- STEDMON C.A., MARKAGER S. & BRO R. (2003) *Marine Chemistry* **82**: 239-54.
- STEELINK C. & TOLLIN G. (1967) "Free radicals in soil" in *Soil Biochemistry* McLaren A.D., Peterson G.M., eds, Marcel Dekker, New York.
- SZAJDAK L., JEZERSKI A. & CABRERA M.L. (2003) *Organic Geochemistry* **34**: 693-700.
- Volume 1: BERTRAND P. (2020) *Electron Paramagnetic Resonance Spectroscopy - Fundamentals*, Springer, Heidelberg.
- YABUTA H. *et al.* (2005) *Geochemistry* **36**: 981-990.